19 ¤ Cantor and Fatou Dusts; Self-Squared Dragons

This chapter takes up two very simple families of nonlinear transformations (mappings) and investigates certain fractal sets which these transformations leave invariant, and for which they can serve as generators.

First, a broken line transformation of the real line deepens our understanding of an old acquaintance, the Cantor dust. These remarks could have been squeezed into Chapter 8, but they are better appreciated at this point.

In particular, they help appreciate the effect of the real and complex quadratic transforms, of the form $x \rightarrow f^*(x) = x^2 - \mu$, where x and μ are real numbers, or $z \rightarrow f^*(z) = z^2 - \mu$, where $z = x + iy$ and μ are complex numbers.

The elementary case $\mu = 0$ is geometrically dull, but other values of μ involve extraordinary fractal riches, many of them first revealed in Mandelbrot 1980n.

The invariant shapes in question are best obtained as a by-product of the study of iteration, that is, of the repeated application of one of the above transformations. The initial values will be denoted by x_0 or z_0, and the k times iterated transforms by f^* will be denoted by x_k or z_k.

Iteration was studied in three rough stages. The first, concerned with complex z, was dominated by Pierre Fatou (1878-1929) and by Gaston Julia (1893-1978). Their publications are masterpieces of classic complex analysis, greatly admired by the mathematicians, but exceedingly difficult to build upon. In my work, of which this chapter is a very concise sketch, some of their basic findings are made intuitive by combining analysis with physics and detailed drawing. And innumerable new facts emerge.

The resulting revival makes the properties of iteration essential to the theory of fractals. The fact that the Fatou-Julia findings did *not* develop to become the *source* of this theory suggests that even classical analysis the needs intuition to develop, and can be helped by the computer.

The intermediate stage includes P. J. Myrberg's studies of iterates of real quadratic mappings of $\mathbb{R}$ (e.g., Myrberg 1962), Stein & Ulam 1964, and Brolin 1965.

The current stage largely ignores the past,

and concentrates on self-mappings of [0,1], as surveyed in Gurel & Rössler 1979, Helleman 1980, Collet & Eckman 1980, Feigenbaum 1981, and Hofstadter 1981. This chapter's last section concerns the exponent δ due to Grossmann & Thomae 1977 and Feigenbaum 1978: the existence of δ is proven to follow from a more perspicuous (fractal) property of iteration in the complex plane.

THE CANTOR DUST CAN BE GENERATED BY A NONLINEAR TRANSFORMATION

We know from Chapter 8 that the triadic Cantor dust $\mathcal{C}$ is invariant by similitudes whose ratio is of the form 3^{-k}. This self-similarity is a vital property, but it *does not* suffice to specify $\mathcal{C}$. In sharp contrast, $\mathcal{C}$ is *entirely* determined as the largest bounded set that is invariant under the following nonlinear "inverted V" transformation:

$$x \to f(x) = \{ \tfrac{1}{2} - |x - \tfrac{1}{2}| \} / r, \text{ with } r = \tfrac{1}{3}.$$

More precisely, we apply this self-mapping of the real axis repeatedly, with x_0 spread out over the x-axis, and the final values reduce to the point $x=-\infty$, plus the Cantor dust $\mathcal{C}$. The fixed points $x=0$ and $x=\frac{3}{4}$ belong to $\mathcal{C}$.

SKETCH OF A PROOF OF THE INVARIANCE OF $\mathcal{C}$. Since $f(x)=3x$ when $x<0$, the iterates of all the points $x_0<0$ converge to $-\infty$ directly, that is, without ceasing to satisfy $x_n<0$. For the points $x_0>1$, direct convergence is preceded by one preliminary step, since $x_k<0$ for all $k\geq 1$. For the points in the gap $\frac{1}{3}<x_0<\frac{2}{3}$, there are 2 preliminary steps, since $x_1>0$ but $x_k<0$ for all $k\geq 2$. For the points in the gaps $1/9<x_0<2/9$ or $7/9<x_0<8/9$, there are 3 preliminary steps. More generally, if an interval is bounded by a gap that is sent to $-\infty$ after k preliminary steps, this interval's (open) mid third will proceed directly to $-\infty$ after the $(k+1)$st step. But *all* the points of $\mathcal{C}$ are found to fail to converge to $-\infty$.

FINITENESS OF THE OUTER CUTOFF

To extend these results to the general Cantor dust with $N=2$ and r between 0 and $\frac{1}{2}$, it suffices to plug in the desired r in $f(x)=\{\frac{1}{2}-|x-\frac{1}{2}|\}/r$. To obtain any other Cantor dust, the graph of $f(x)$ must be an appropriate zigzag curve.

However, no comparable method is available for the Cantor dust extrapolated to the whole real axis. This is a special case of a very general feature: Typically, a nonlinear $f(x)$ carries *within itself* a finite outer cutoff Ω. To the contrary, as we know well, all linear transformations (similarities and affinities) are characterized by $\Omega=\infty$, and a finite Ω (if one is required) must be imposed artificially.

ANATOMY OF THE CANTOR DUST

We know from Chapter 7 that $\mathcal{C}$ is a very "thin" set, yet the behavior of the iterates of $f(x)$ leads to a better understanding of fine

distinctions between its points.

Everyone must be tempted, at first acquaintance, to believe that $\mathcal{C}$ reduces to the end points of the open gaps. But this is very far from being the case, because $\mathcal{C}$ includes by definition all the limits of sequences of gap end points.

This fact is *not* reputed intuitive. With many fellow students, I would have agreed if our battered acquaintance Hans Hahn had listed these limit points among the concepts whose existence must be imposed by cold logic. But the present discussion yields *intuitive* proof that these limit points have strong and diverse personalities.

For example, the point $x=\frac{3}{4}$, which $f(x)$ leaves unchanged, lies neither within any mid third interval, nor on its boundary. Points of the form $x=(\frac{1}{4})/3^k$ have iterates that converge to $x=\frac{3}{4}$. In addition, there is an infinity of limit cycles, each made up of a finite number of points. And $\mathcal{C}$ also contains points whose transforms run endlessly around $\mathcal{C}$.

THE SQUARING GENERATOR

The inverted V generating function $f(x)$ used in the preceding sections was chosen to yield a familiar result. But it makes the Cantor dust seem contrived. Now we replace it by

$$x \to f(x) = \lambda x(1-x),$$

whose unexpected wealth of properties was first noted in Fatou 1906. Changing the origin and the scale of the x, and writing $\mu=\lambda^2/4-\lambda/2$, this function can be written as

$$x \to f^*(x) = x^2-\mu.$$

Convenience is served by using sometimes $f(x)$, and sometimes $f^*(x)$.

It is nice to call $f(x)$ or $f^*(x)$ the *squaring generator*. Squaring is, of course, an algebraic operation, but it is given a geometric interpretation here, so that the sets it leaves invariant can be called *self-squared*. Strict squaring replaces the point of abscissa x by the point of abscissa x^2. Thus, the self-squared points on the line reduce to $x=\infty$, $x=0$, and $x=1$. The addition of $-\mu$ may seem totally innocuous, but in fact it introduces totally unexpected possibilities we now consider.

FATOU'S REAL SELF-SQUARED DUSTS

Having yielded a familiar end product, the Cantor dust, the V transformation makes an extraordinary but never widely known discovery of Pierre Fatou easier to state. Fatou 1906 assumes that λ is real and satisfies $\lambda>4$, and he investigates the largest of the bounded sets on $\mathbb{R}$, that are left invariant under $f(x)$. This is a close relative to the Cantor dust, which I call *real Fatou dust*. It requires no further explanation, and is illustrated in Plate 192.

In the complex plane, the largest bounded self-squared set, for the above λ's, remains the real Fatou dust.

SELF-SQUARED JULIA CURVES IN THE PLANE (MANDELBROT 1980n)

The simplest self-squared curve is obtained for $\mu=0$: it is the circle $|z|=1$. By the transformation $z \to z^2$, a belt wound *once* around the circle stretches into a belt wound *twice*, the "buckle" at $z=1$ remaining fixed. The corresponding largest bounded self-squared domain is the disc $|z| \leq 1$.

However, introducing a real $\mu \neq 0$ (Plates 186 and 187), then a complex μ (Plates 190 and 191), opens Pandora's boxes of possibilities, the *Julia fractal curves*. They satisfy the eye no less than they satisfy the mind.

THE SEPARATOR $\mathcal{S}$. The topology of the largest bounded self-squared set depends on where μ lies with respect to a ramified curve $\mathcal{S}$, which I discovered and now call *separator*. It is the connected boundary of the black shape in bottom Plate 188 ; it is a "limit lemniscate," namely the limit for $n \to \infty$ of the algebraic curves called lemniscates, defined by $|f_n^*(0)|=R$ for some large R. See Plate 189 for the structure of $\mathcal{S}$.

THE ATOMS. The open domain within $\mathcal{S}$ splits into an infinity of maximal connected sets I now propose to call "atoms." Two atoms' boundaries either fail to overlap, or have in common one point, to be called "bond," that belongs to $\mathcal{S}$.

TOPOLOGICAL DIMENSION. When μ lies outside $\mathcal{S}$, the largest bounded self-squared set is a (Fatou) dust. When μ lies within $\mathcal{S}$, or is a bond, the largest such set is a domain bounded by a self-squared curve. At least some μ on $\mathcal{S}$ yield a tree-like curve.

SELF-SQUARED FRACTALS. These dusts and curves being fractal when $\mu \neq 0$ is rumored to have been proven fully in some further cases by Dennis Sullivan, and I harbor no doubt it will be proven in all cases.

The shape of a self-squared dust or curve varies continuously with μ, hence D is bound to be a smooth function of μ.

RAMIFICATION. When λ lies in one of the open empty discs of top Plate 189, the self-squared curve is a closed simple curve (not ramified, a loop), as in Plates 186 and 187.

When λ lies on the circles $|\lambda|=1$ or $|\lambda-2|=1$, or in the surrounding open connected region, the self-squared curve is a ramified net, with tremas bounded by fractal loops, like the dragons in Plate 191.

When λ lies in the very important island molecules, which will soon prove to be *regions of nonconfluence to* 1, the self-squared curve is either a σ-loop, or a σ-dragon, as in bottom Plate 190. The σ introduces no new loop.

μ-ATOMS AND μ-MOLECULES

To dissect the parameter map further is easier when the parameter is μ. A μ-atom may be heart-shaped, in which case it is the "seed" to which an infinity of oval-shaped atoms bind either directly or through intermediate atoms. Mutually bound atoms, plus their bonds, form a "molecule." A seed's cusp is never a bond.

To each atom is attached an integer w, its "period." When μ lies in an atom of period w,

the iterates $f_n^*(z)$ converge to ∞ or to a stable limit cycle containing w points. Within an atom of period w, $|f_w^{*\prime}(z_\mu)|<1$, where z_μ is any point of the limit cycle corresponding to μ. On the atom's boundary, $|f_w^{*\prime}(z_\mu)| = 1$, with $f_w^{*\prime}(z_\mu) = 1$ characterizing a cusp or a "root." Each atom contains a point to be called "nucleus," satisfying $f_w^{*\prime}(z_\mu) = 0$ and $f_w^*(0) = 0$.

The nuclei on the real axis were introduced by Myrberg (see Myrberg 1962), and rediscovered in Metropolis, Stein & Stein 1973. The corresponding maps are often called "superstable" (Collet & Eckman 1980).

Viewed as algebraic equation in μ, $f_w^*(0) = 0$ is of order 2^{w-1}. Hence, there could be at most 2^{w-1} atoms of period w, but there are fewer, except for w=1. For w=2, $f_2^*(0) = 0$ has 2 roots, but one of them is already the nucleus of an "old" atom of period 1. More generally, all the roots of $f_m^*(0) = 0$ are also roots of $f_{km}^*(0) = 0$ where k is an integer > 1. Next, observe that each rational boundary point on the boundary of an atom of period w, defined as satisfying $f_w^{*\prime}(z_\mu) = \exp(2\pi i m/n)$, where m/n is an irreducible rational number <1, carries a "receptor bond" ready to connect to an atom of period nw. As a result, some new atoms bind to existing receptor bonds. But not all new atoms are thereby exhausted, and the remaining ones have no choice but to seed new molecules. The molecules are therefore infinite in number.

When μ varies continuously in a molecule, each outbound traversal of a bond leads to bifurcation: w is multiplied by n. Example: increasing a real-valued μ leads to Myrberg's period doubling. The inverse of bifurcation, which Mandelbrot 1980n investigates and calls *confluence*, must stop at the period of the molecule's seed. The continent molecule is the region of confluence to c=1, and each island molecule is a region of confluence to c>1. The dragon's or sub-dragon's shape is ruled by the values of $f_w^{*\prime}(z_\mu)$ and w/c.

THE SEPARATOR IS A FRACTAL CURVE; FEIGENBAUM'S δ AS A COROLLARY

I conjecture ◅ via a "renormalization" argument ► that atoms increasingly removed from their molecule's seed come increasingly close to being *identical* in shape.

A corollary is that the boundary of each molecule is locally self-similar. Since it is not smooth on small scales, it is a fractal curve.

This local self-similarity generalizes a fact concerning Myrberg bifurcation, due to Grossmann & Thomae and to Feigenbaum. The widths of increasingly small sprouts' intercepts by the real axis of λ or μ, converge to a geometrically decreasing sequence, of ratio δ=4.66920... (Collet & Eckman 1980). In its original form, the existence of δ seems a technical analytic result. Now it proves to be an aspect of a broader property of fractal scaling.

Each bifurcation into m>2 introduces an additional basic ratio. ■

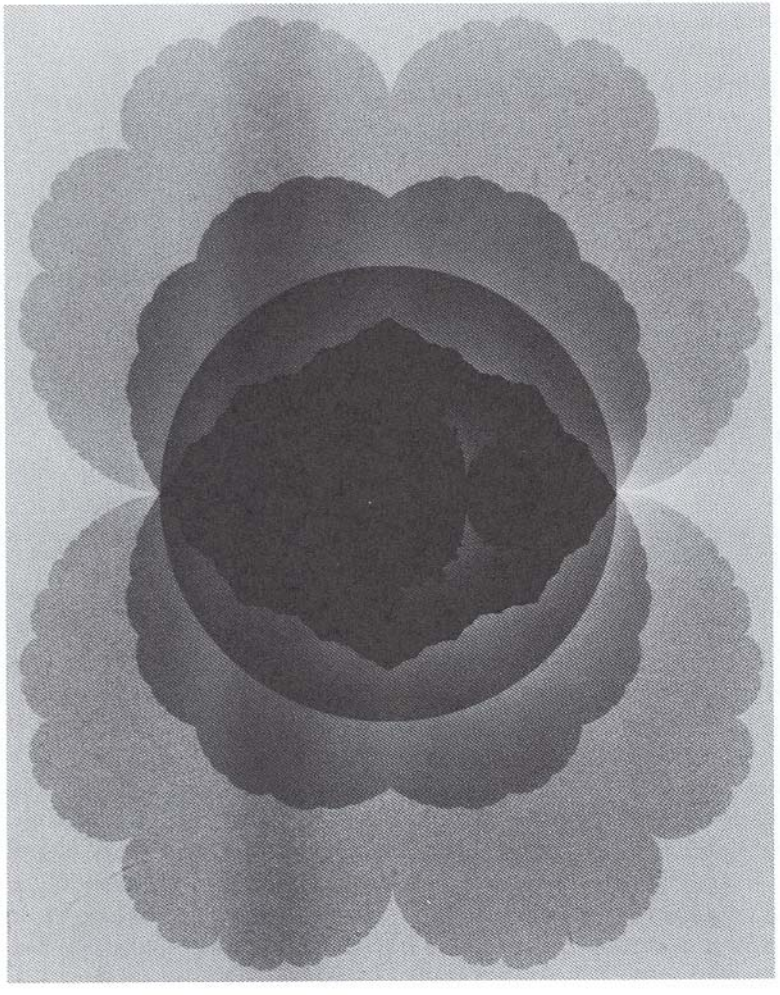

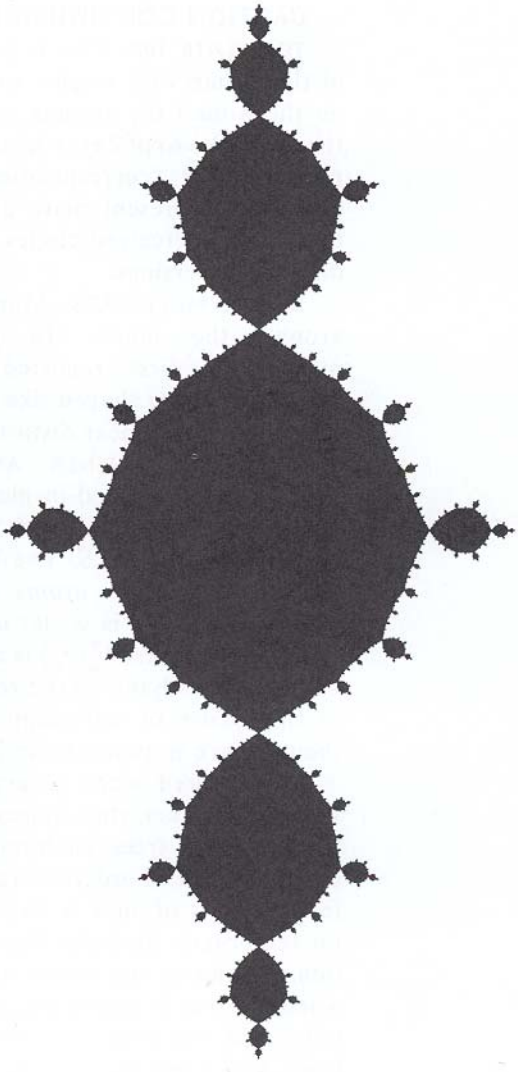

Plate 185 ¤ SELF-SQUARED FRACTAL CURVES FOR REAL λ

The shapes in Plates 185 to 192 are presented here for the first time, except for a few that are reproduced from Mandelbrot 1980n.

The left side of this plate represents the maximal bounded self-squared domains for λ = 1, 1.5, 2.0, 2.5 and 3.0. The central black shape spans the segment [0,1].

λ=1: SCALLOP SHELL.

λ=3: SAN MARCO DRAGON CURVE. This is a mathematician's wild extrapolation of the skyline of the Basilica in Venice, together with its reflection in a flooded Piazza; I nicknamed it the *San Marco dragon*.

The right side of this plate is relative to λ=3.3260680. This is the nuclear λ (as defined on p. 184) corresponding to w=2. The corresponding self-squared shape is turned by 90° to make it fit in. ■

CAPTION CONTINUED FROM P. 188

TOP PLATE 188. This is part of the inverse of the λ-map with respect to $\lambda=1$. Examining on the λ-map the sprouts whose roots are of the form $\lambda=\exp(2\pi i/n)$, one gains the impression that "corresponding points" lie on circles. The present plate provides confirmation. Other perceived circles are confirmed by different inversions.

ISLAND MOLECULES. Many of the "spots" around the maps are genuine "island molecules," first reported in Mandelbrot 1980n. They are shaped like the whole μ map, except for a nonlinear distortion.

SEPARATOR, SPINES AND TREES. The boundary of the filled-in black domain in the λ- or μ map is a connected curve I discovered and call *separator* $\mathcal{S}$. The set within $\mathcal{S}$ decomposes into open *atoms* (see text). When the atom's period is w, let us define its *spine* as the curve where $f^{*}_{w}(z_{\mu})$ is real.

The spines lying on the real axis are known in the theory of self-mapping as $[0,1]$, and their closure is known to be $[-2,4]$.

I discovered more generally that the closure of the other atom spines decomposes into a collection of trees, each rooted on a receptor bond. The list of orders of ramification at different points of such a tree is made up of 1 for the branch tips, plus the orders of bifurcation leading to the tree's root. Furthermore, when the tree is rooted on an island atom, one must add the orders of bifurcation leading from $|\lambda-2|\leq 1$ or $|\lambda|\leq 1$ to this atom.

BOTTOM LEFT PLATE 189. This is a detailed λ map near $\lambda=2-\exp(-2\pi i/3)$. The set within $\mathcal{S}$ is the limit of domains of the form $|f_n(\frac{1}{2})|<R$, whose boundaries are algebraic curves called lemniscates. A few such domains are shown here in superposition. For large n, these domains seem disconnected, and so does the λ map, but in fact they connect outside the grid used in the computation.

BOTTOM RIGHT PLATE 189. This is a detailed λ map near $\lambda=2-\exp(-2\pi i/100)$. This hundred-fold branching tree shares striking features with the z map in Plate 191. ■

Plate 187 ¤
COMPOSITE OF SELF-SQUARED FRACTAL CURVES FOR REAL λ

This draped "sculpture" was made within a computer's memory, by a process that amounts to whittling away all points in an initial cube, whose iterates by $z\rightarrow\lambda z(1-z)$ converge to infinity. The parameter λ is a real number ranging from 1 to 4. The λ axis runs vertically along the sculpture's side. And x and y form the complex number $z=x+iy$.

Each horizontal section is a maximal bounded self-squared shape of parameter μ.

For the special value $\lambda=2$, this section's boundary is a circle: the drape's "belt."

For all other values of λ, the self-squared shape's boundaries are fractal curves, including those shown in Plate 185. One perceives striking "pleats" whose position varies continuously with λ; they are pressed *in* below the belt, and pressed *out* above the belt.

Of special interest are the blobs on the wall holding the drape. This sculpture cannot possibly do justice to the complication of the top of the drape. A) For every value of λ, the drape includes, as "backbone," a fractal tree formed by the iterated pre-images of the x-interval $[0,1]$. For all small, and some high values of $\lambda<3$, this tree's branches are completely "covered by flesh." For other high values of λ, however, there is no flesh. The branches along either $x=\frac{1}{2}$ or $y=0$ are visible here, but the graphic process unavoidably misses the rest. B) Certain horizontal stripes of the wall behind the drape are entirely covered with tiny "hills" or "corrugations," but only a few of the largest ones can be seen. These stripes and hills concern the "island molecules" (Plates 188 and 189) intersected by the real axis. Observations A) and B) generalize the Myrberg-Feigenbaum theory. ■

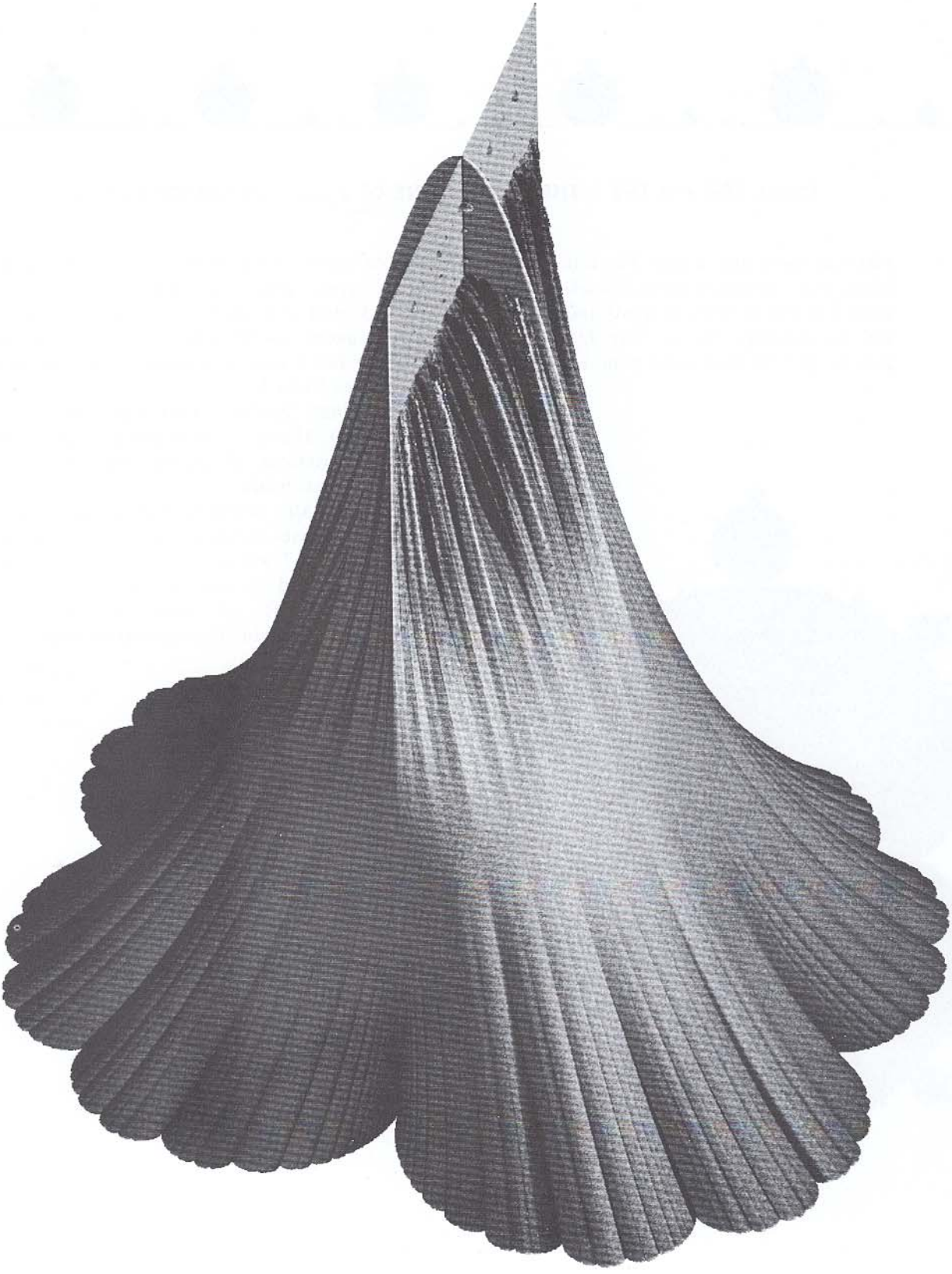

Plates 188 and 189 ⌑ THE SEPARATORS OF $z \to \lambda z(1-z)$ AND OF $z \to z^2-\mu$

BOTTOM PLATE 188. μ-MAP. The μ in the closed black area (bounded by a fractal curve) are such that the iterates of $z_0=0$ under $z \to z^2-\mu$ fail to converge to ∞. The large cusp is $\mu=-\frac{1}{4}$, and the right-most point is $\mu=2$.

TOP PLATE 189. λ-MAP. The λ in the closed black area, plus the empty disc, satisfy $\mathrm{Re}\lambda>1$ and are such that the iterates of $z_0=\frac{1}{2}$ under $z \to \lambda z(1-z)$ fail to converge to ∞. The full λ map is symmetric with respect to the line $\mathrm{Re}\lambda=1$.

THE DISC $|\lambda-2|\leq 1$, AND THE DISC $|\lambda|\leq 1$ LESS $\lambda=0$. The λ in these domains are such that the iterates of $z_0=\frac{1}{2}$ converge to a bounded limit point.

CORONA AND SPROUTS. The λ-map outside the empty discs forms a "corona." It splits into "sprouts," whose "roots" are "receptor bonds" defined as the points of the form $\lambda=\exp(2\pi i m/n)$ or $\lambda=2-\exp(2\pi i m/n)$, with m/n an irreducible rational number <1.

CAPTION CONTINUES ON P. 186

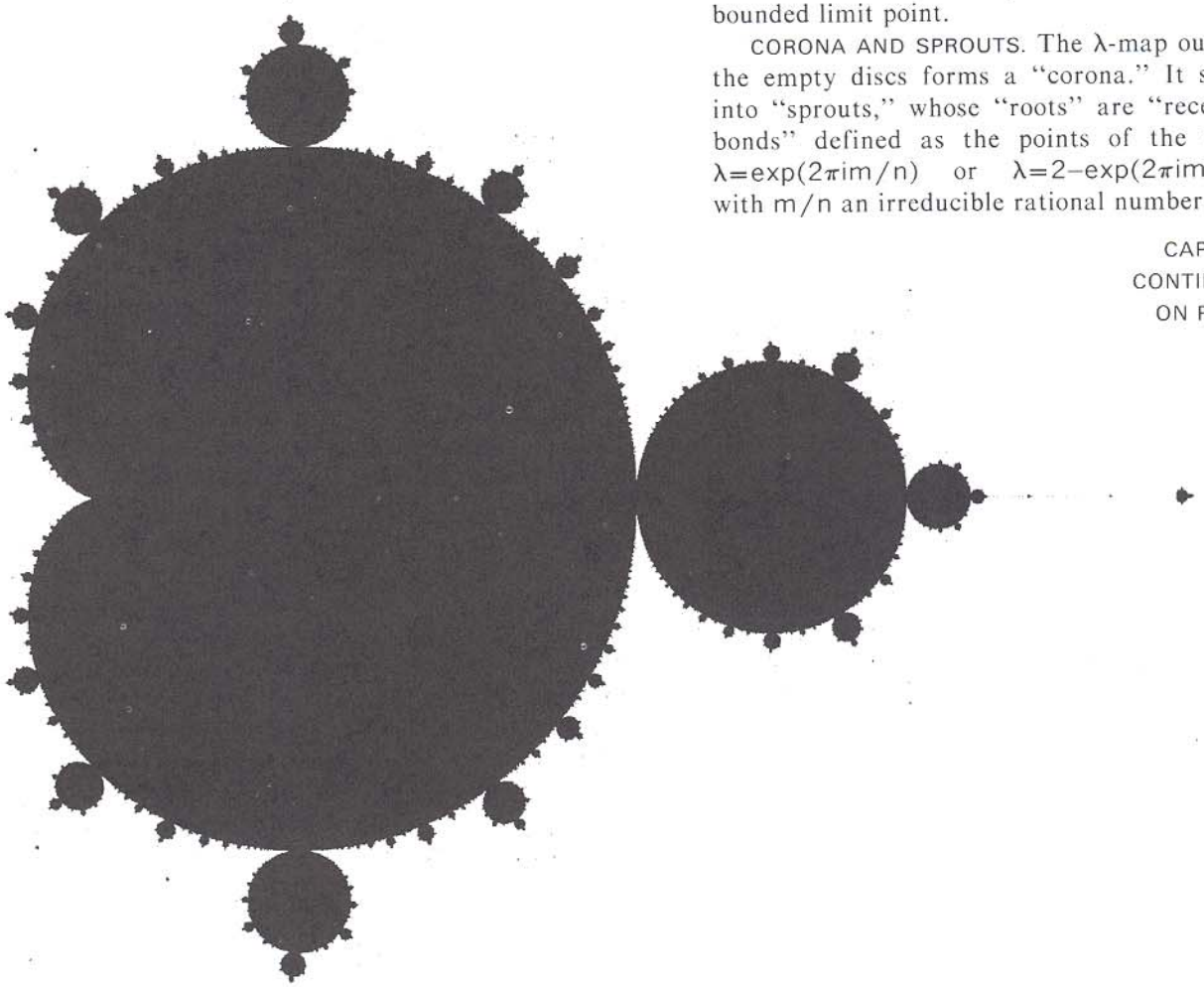

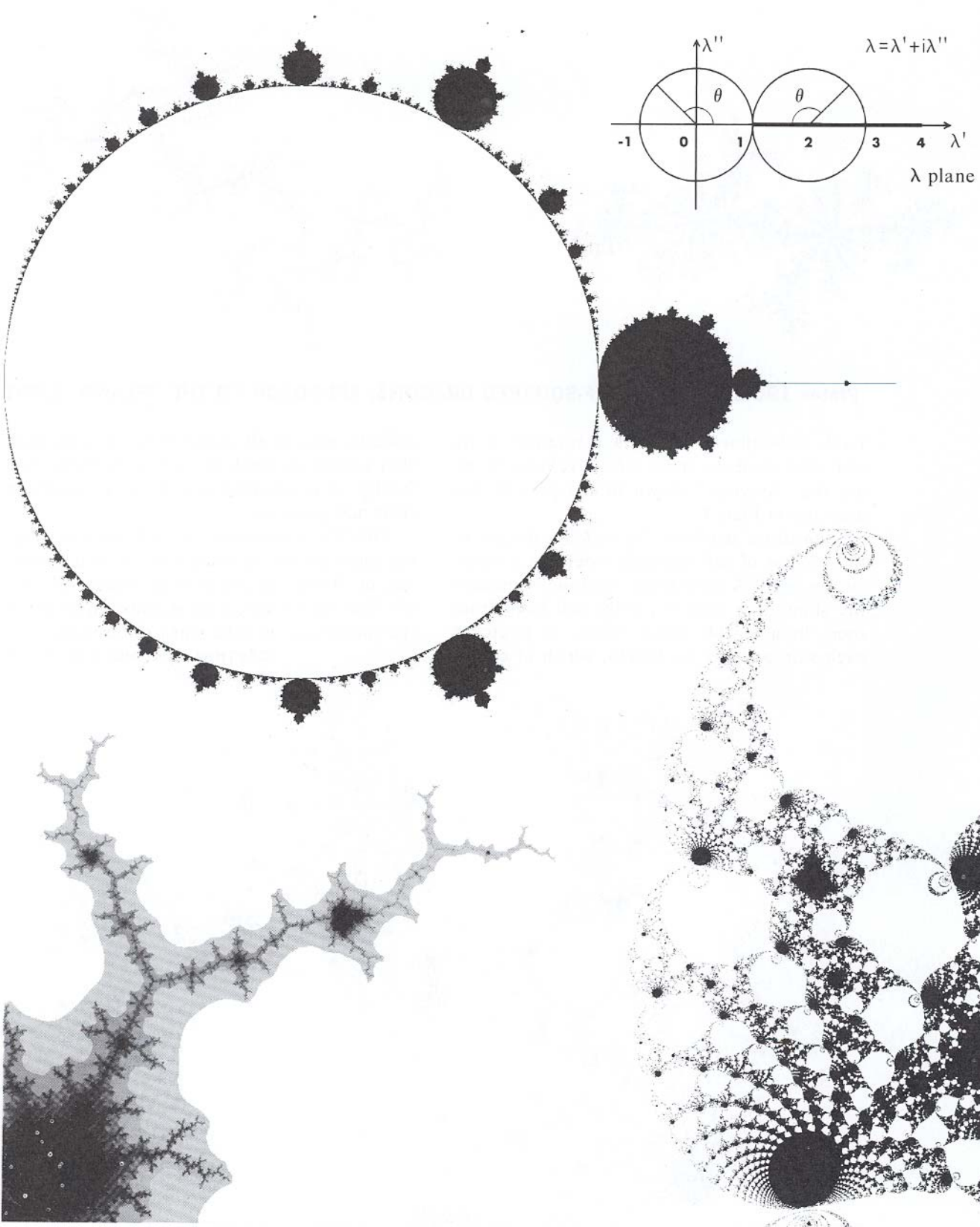
λ''
λ=λ'+iλ''
θ
θ
-1
0
1
2
3
4
λ'
λ plane

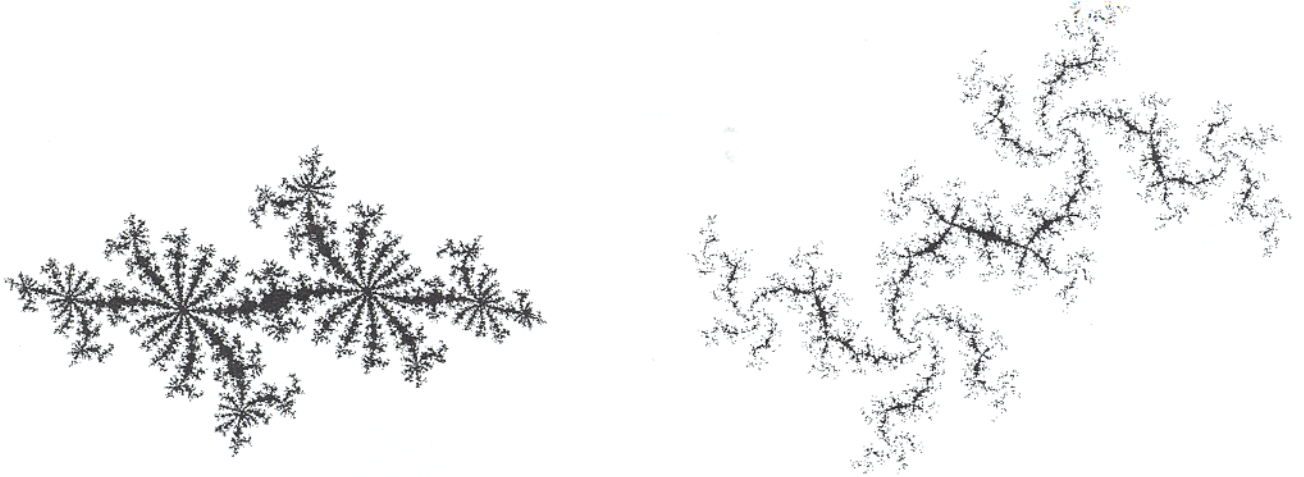

Plates 190 and 191 ¤ SELF-SQUARED DRAGONS; APPROACH TO THE "PEANO" LIMIT

Each self-squared curve is attractive in its own way. And the most attractive ones to me are the "dragons" shown in the present figures and in Plate C5.

DRACONIC MOLTING. To watch a dragon in the process of self-squaring would be a fascinating sight! A monstrous "molting" detaches the skins of a dragon's belly and back from their innumerable folds. Then, it stretches each skin to twice its length, which of course remains infinite all along! Next, it folds each skin around the back as well as the belly. And finally, it re-attaches all the folds neatly in their new positions.

FRACTAL HERALDRY. The self-squared dragons must not be confused with the self-similar one of Harter & Heightway, Plates 66 and 67. The reader may find it amusing to detail the similarities and the many differences.

CAPTION CONTINUES ON P. 192

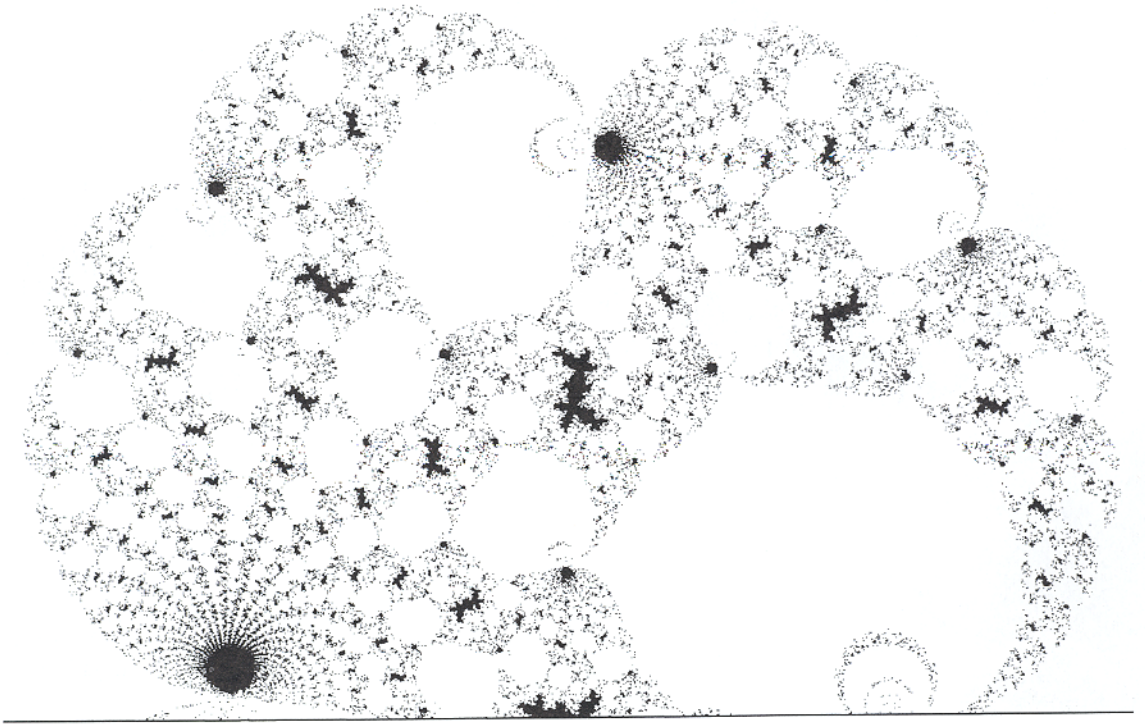

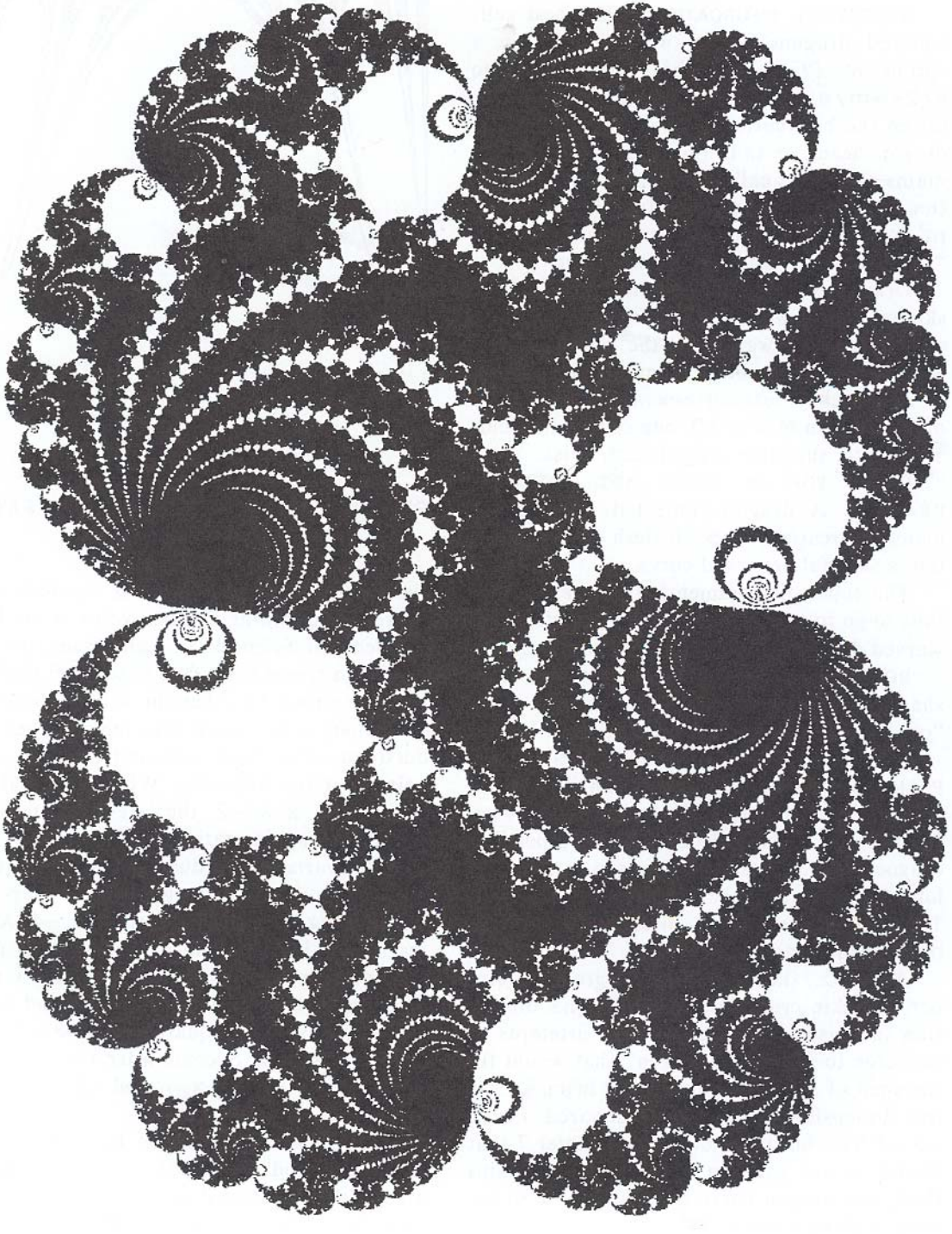

CAPTION CONTINUED FROM P. 190

SUCCESSIVE BIFURCATIONS. The best self-squared dragons obtain where λ lies in a sprout of Plate 189 that corresponds to $\theta/2\pi=m/n$, with small integers n and m. Given the bifurcation order n, the number of dragon heads or tails (or whatever these domains should be called) around each articulation point is n. A second bifurcation of order m'/n' splits each of these domains into n' "sausage links," and thins them down.

Dragons with a nice heft, neither obese nor skinny, obtain when λ lies within a sprout, at some distance away from the root. Dragons with a nice twist obtain when λ lies near one of the 2 subsprouts corresponding to an order of bifurcation of 4 to 10: one subsprout yields a leftward, the other a rightward, twist.

RIGHT TOP OF PLATE 190. "STARVED DRAGON." A dragon subjected to infinitely many bifurcations loses all flesh and collapses into a skeletal branched curve.

The topological dimension of the set that fails to go to ∞ is 0 for the Fatou dusts, 1 for starved dragons, and 2 for other dragons.

BOTTOM OF PLATE 190. σ-DRAGON. This shape is connected; its λ lies in the large "offshore island" in bottom right Plate 189.

PLATE 191. THE SINGULAR LIMIT $\lambda=1$. PEANO DRAGONS. Let λ lie in an island offshore of the bond at $\theta=2\pi/n$. As $n\to\infty$, $\theta\to 0$, hence λ tends to 1. The corresponding dragon must necessarily converge to the scallop shape at the base of the drape in Plate 187. But a qualitative difference separates $n=\infty$ from n large but finite.

As $n\to\infty$, the dragon's arms grow in number, the skin crumples, and the skin's dimension increases. The whole really attempts to converge to a "hermit-dragon" that would fill the shell of a $\lambda=1$ scallop to the brim, i.e., to the dimension $D=2$. A self-squared Peano curve? Yes, but we know from Chapter 7 that Peano curves are not curves: as it attains $D=2$, our dragon curve dies as a curve to become a plane domain. ■

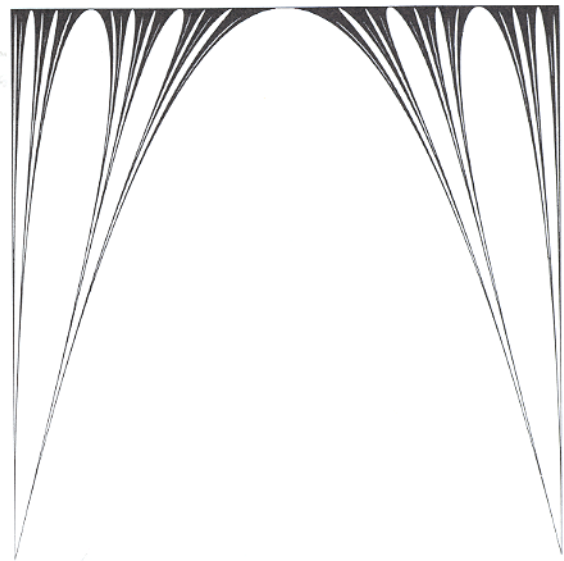

Plate 192 ¤ REAL SELF-SQUARED FATOU DUSTS ON [0,1]

Fatou 1906 is a masterpiece of an odd literary genre: the *Comptes Rendus Notes* of the Paris Academy of Sciences. In many cases, the purpose is to reveal little, but to squirrel evidence that the author had thought of everything.

Among other marvelous remarks best understood after long self-study, Fatou 1906 points out the following. When λ is real and either $\lambda>4$ or $\lambda<-2$, the largest bounded set that the transformation $x\to f(x) = \lambda x(1-x)$ leaves invariant is a dust contained in $[0,1]$. This plate illustrates this dust's shape for $\lambda>4$. Along the vertical coordinate, $-4/\lambda$ varies from -1 to 0. The black intervals mark the end points of the tremas of order 1 to 5. The end points x_1 and x_2 of the mid trema are solutions of the equation $\lambda x(1-x)=1$; they draw a parabola. Second-order tremas end at the points $x_{1,2}$, $x_{1,2}$, $x_{2,1}$, and $x_{2,2}$, such that $\lambda x_{m,n}(1-x_{m,n}) = x_m$, etc.

The remarkable relation between Cantor-like dusts and one of the most elementary among all functions deserves to be known beyond the circle of specialists. ■